ELSEVIER

Biochimica et Biophysica Acta 1185 (1994) 103–111

BBA Biochimica et Biophysica Acta

A XANES study of the manganese complex of inhibited PS II membranes indicates manganese redox changes between the modified S_1, S_2 and S_3 states

Dugald J. MacLachlan, Jonathan H.A. Nugent *, Michael C.W. Evans

Department of Biology, Darwin Building, University College London, Gower Street, London WC1E 6BT, UK

(Received 29 June 1993)

Abstract

Manganese K-edge X-ray spectra have been obtained for Photosystem II samples treated to inhibit oxygen evolution without displacement of manganese. Inhibition treatments included the use of ammonia, acetate and high concentrations of sodium chloride. These treatments affect the binding of calcium and chloride cofactors and result in either a block or slowing of OEC S-state cycling at the $S_3 \rightarrow S_0$ transition. Following each inhibition treatment the S-states show characteristic K-edge energies and EPR spectra. The differences between each type of inhibitory treatment in the K-edge energy for each S-state may result from conformational and/or ligand changes to the manganese complex. However for each of the inhibitory treatments, the K-edge energies showed edge shifts between S-states consistent with manganese oxidation on both the $S_1 \rightarrow S_2$ and $S_2 \rightarrow S_3$ transitions.

Key words: Photosystem II; Oxygen evolving complex; Manganese complex; XANES

1. Introduction

Water oxidation in cyanobacteria, algae and higher plants is carried out by the membrane–protein complex termed Photosystem II (PS II) (see [1,2] for reviews). At the heart of the complex is a reaction centre made up of two membrane-spanning proteins, D1 and D2. These bind the components necessary for charge separation and stabilisation, a situation analogous to the L and M subunits of the structurally characterised purple non-sulphur bacteria. The reaction is initiated by the absorption of a photon by P680, a chlorophyll species, and leads to charge separation between P680 and a pheophytin, the primary electron acceptor. Charge separation and stabilisation on the electron acceptor side of P680 is continued by electron transport from the pheophytin to quinones Q_A, Q_B and on to a membrane pool of plastoquinones. Electrons are donated to $P680^+$ by a redox active tyrosine, Y_Z. Y_Z^+ is in turn reduced by a manganese cluster. Water oxidation requires four turnovers of the reaction centre. The oxidising equivalents are thought to be mainly stored on the manganese complex, which is also thought to be the site of water oxidation. There are five different redox states, $S_i = 0$–4, and the water oxidising enzyme is termed the oxygen evolving complex (OEC).

Inorganic cofactors, calcium and chloride, are necessary for maximal OEC activity [3,4]. Calcium has been shown to occur in different binding sites in PS II. The population of calcium binding sites are divided into at least two groups; one high affinity site ($K_d = 10$–130 μM) and one low affinity site ($K_d = 0.3$–1 mM), [1,2]. The latter is thought to be associated with a functioning S_3 to S_0 transition. The treatment of PS II membranes with 1–2 M NaCl or citrate at pH 3, results in

* Corresponding author. Fax: +44 71 3807096.

Abbreviations: Chl, chlorophyll; EPR, electron paramagnetic resonance spectroscopy; EXAFS, extended X-ray absorption fine structure; Hepes, 4-(2 hydroxyethyl)-1-piperazine ethanesulphonic acid; Hpp, peak to trough linewidth of EPR spectrum; MES, 2-(*N*-morpholino)ethanesulfonic acid; OEC, oxygen evolving complex; PPBQ, phenyl-1,4-benzoquinone; PS II, Photosystem II; XANES, X-ray absorption near edge structure.

SSDI 0005-2728(93)E0210-H

the loss of oxygen evolution which may be recovered by addition of Ca^{2+}, or to a lesser extent Sr^{2+} [5,6]. Chloride is also thought to bind in two or three different sites in PS II. One site is thought to be at or close to the manganese cluster. Depletion of chloride gives an inhibition of OEC turnover and the resulting changes in EPR, fluorescence and thermoluminescence properties indicate a block at the $S_2Y_Z^+$ or S_3 to S_0 transition [2,7].

As the OEC cycles through the different S-states, oxidation of the manganese cluster results in characteristic EPR signals. The EPR signal from intact PS II membranes poised in the S_2 state is a multiline, with 18–20 lines spread over 160 mT around $g = 2$ [8]. EPR signals attributed to the OEC in the S_2 state have also been observed in PS II treated by NaCl washing or pH 3 citrate treatment [9–11]. These treatments result in a dark stable multiline signal ($g = 1.98$, > 20 lines spread over 160 mT, $t_{\frac{1}{2}}$ several hours) which is lost on addition of calcium and is assigned to a chelator modified S_2 state [12]. Illumination at 273 K followed by freezing these treated samples to 77 K results in loss of the modified multiline and the generation of a split EPR signal (Hpp 13.0–16.5 mT) near $g = 2$ [9–11]. This was assigned to the S_3 state [9], which was supported by experiments showing the appearance of the signal following a single laser flash to a sample in the modified S_2 state [13]. The 'S3' signal was also observed in PS II from the cyanobacterium, *Synechocystis* following washes in Ca^{2+}-free buffer containing EGTA [14] and in *Phormidium laminosum* (unpublished results).

'S3' type EPR signals were also observed in chloride-depleted or fluoride-treated preparations [15,16] and in ammonia-treated PS II [17,18]. The 'S3' type signals found in these samples have decreased splitting, < 10 mT, which indicates different structural properties between these and PS II samples formed by treatment with 1–2 M NaCl or citrate at pH 3. Recently, acetate treatment has been shown to result in an 'S3' signal with an increased linewidth, Hpp 24.0 mT, and additional peaks [19,20].

It has been suggested that during the $S_2 \rightarrow S_3$ transition, oxidation of a histidine residue occurs close to the manganese cluster. It was proposed that the interaction between oxidised histidine and the manganese cluster gave the 'S3' EPR signal [13]. This might occur (i) as part of the normal S-state transition, or (ii) as an auxiliary reaction, resulting from impairment of the normal S_2 to S_3 transition by calcium depletion [11]. Boussac et al. [13] correlated their EPR data to the oxidation of a histidine residue using transient absorption spectroscopy. Hallahan et al. [17] have suggested that an interaction between Y_Z^+ and S_2 may account for the 'S3' signal, based on the observation of an increased stability of Y_Z^+ in the inhibited samples they studied.

X-Ray absorption studies have provided structural information on the manganese complex. Mn K-edge studies have indicated an overall lower oxidation state or conformational changes in the S_1 state in 1–2 M NaCl or pH 3 citrate washed samples compared to that in normal PS II particles [19,21,22]. Comparison of Mn K-edge energies of untreated samples poised in the different S-states has provided evidence for Mn redox changes during S-state transitions. The data has been interpreted as being consistent with the oxidation of Mn on the transitions, $S_0 \rightarrow S_1$ [23,24], $S_1 \rightarrow S_2$ [22,23,25,26], but not on $S_2 \rightarrow S_3$ [25,27]. Such an interpretation has been supported by measurements of the S-state dependent relaxation enhancement for the redox active tyrosine Y_D [28,29], proton NMR relaxation [30] and some, but not all, optical data (see [1] for review).

Recent re-examination of Mn oxidation in the OEC using intact PS II membranes, poised in each S-state by flash excitation, has revealed Mn K-edge shifts consistent with oxidation changes on each of the native S-state transitions [31]. In this paper we examine the electronic changes occurring in samples inhibited on the $S_3 \rightarrow S_0$ transition.

2. Materials and methods

PS II membranes (BBYs, Chl *a*/Chl *b* ratio 2.0–2.2 : 1 [32]) were prepared from market spinach by the method of Ford and Evans [33]. Buffers and sucrose were treated with Chelex to remove any calcium impurities. All samples were stored at 77 K before use. The experiments were repeated using a different PS II preparation on each occasion.

Sodium acetate, sodium chloride or ammonium chloride treated PS II was prepared from PS II membranes by a simple procedure. Membranes were first exchanged into the required pH buffer by centrifugation ($40\,000 \times g$ for 30 min) and resuspension. 40 mM MES (pH 5.5) was used for acetate treatment, 40 mM MES (pH 6.0) for sodium chloride treatment and 20 mM Hepes (pH 7.5) for ammonia treatment. The membranes were then centrifuged at $40\,000 \times g$ for 30 min and resuspended in the final buffer containing the reagent concentrations and at the pH given in the text (see also [17,20]). All final buffers contained 0.3 M sucrose. 0.5 mM PPBQ was added to samples that were to be illuminated. Samples for X-ray absorption studies were centrifuged at $260\,000 \times g$ for 1 h and loaded into polycarbonate holders [22]. The properties of the sodium chloride-treated preparation were very similar to those of 'calcium-depleted' samples [1,2,9–13] in that the same EPR signals are observed for the S_2 and 'S3' states and calcium chloride addition restores high levels of activity. Studies using the effects of high

concentrations (> 100 mM) of acetate and ammonium ions have been reported previously ([see 1,2,20,34]).

The membranes obtained and used as a result of the treatments described were depleted of greater than 90% of their oxygen evolving activity (measured in a Clark-type oxygen electrode at 298 K using, as control, depleted membranes to which 20 mM calcium chloride was added and incubated for 30 min). Control values were 350–600 μmol O_2/mg Chl/h. Calcium chloride treatment restored high levels of oxygen evolution. Measurements taken from samples following X-ray spectroscopy gave > 80% the activity of control samples not exposed to the X-ray beam.

The simple high salt procedure was used because it enabled a better comparison between the salt treatments, simplified sample preparation without a significant change in properties and minimised exposure to light ensuring retention of a modified S_1 state. Dialysis of the treated samples to reduce the salt concentration as in the calcium depletion procedure given in [9,17] gave samples with identical EPR and oxygen evolution properties. It was, however, difficult during dialysis and centrifugation (1) to eliminate exposure to light, allowing formation of dark stable S_2 (detected by EPR) in significant amounts, and (2) to obtain samples free of contaminating Mn^{2+}. Centrifugation of the treated samples at 40 000 × g for 30 min without dialysis followed by SDS polyacrylamide gel electrophoresis of the pelleted material, showed that the 17 kDa and 23 kDa extrinsic polypeptides are released by the high salt concentrations (600 mM) as expected (see [1] for review of effects of high salt concentrations).

Preparation of samples in different S-states

All procedures were carried out in the dark or in the presence of a dim green light, producing samples initially in the S_1 state, as indicated by the absence of a multiline EPR signal for the ammonia and sodium chloride-treated samples (acetate-treated samples do not exhibit a multiline signal [20]). S_1 samples were then frozen in the dark. To obtain the 'S3' EPR signal, samples were illuminated on each side at 277 K for 1 min (total 2 min) using an unfiltered 650 W light source (1000 $\mu E/m^2/s$) and then frozen to 77 K under illumination. Samples formed by this procedure do not contain more than 15% of the maximum S_2 multiline intensity. S_2 was generated by storing illuminated samples on ice at 273 K for 5 or 10 min in the dark, before freezing to 77 K. In the case of ammonium chloride- and sodium chloride-treated samples, the amount of S_2 multiline EPR signal formed was > 90% that of a sample containing 0.5 mM DCMU that was illuminated directly from S_1 to S_2. Illumination treatments for EPR and EXAFS samples were carried out immediately before measurement. The type of X-ray spectroscopy performed use X-ray fluorescence measurements, so that although high concentrations of sample are used, measurements are from thin samples (typically several-fold less than EPR samples) and light limitation was unlikely to occur in the illumination regimes employed. However, samples of identical concentration were checked by EPR to ensure that illumination produced identical changes in modified S state in both EPR and EXAFS samples.

EPR spectrometry

For EPR at cryogenic temperatures, 0.3 ml samples (at > 10 mg Chl/ml) were placed in 3 mm diameter EPR tubes or samples at EXAFS concentration (> 50 mg Chl/ml) were made using specially adapted holders. EPR spectrometry was performed using a Jeol RE1X spectrometer fitted with an Oxford Instruments liquid helium cryostat. EPR conditions are given in the figure legends. Spectra were recorded and manipulated using a Dell microcomputer running Asyst software. Ideally EPR and EXAFS measurements should be done on the same sample with EPR being carried out immediately before and after EXAFS measurements. Facilities for EPR at cryogenic temperature are unavailable at Daresbury, therefore EXAFS and then EPR samples were made for each treatment from the same preparation. Making the EPR samples immediately after the EXAFS samples ensured any sample deterioration was noted. EPR samples were also taken from the EXAFS sample following EXAFS or XANES measurements. This procedure provided monitoring of EXAFS sample condition and avoided problems of decay of higher S states that might have occurred between EXAFS and EPR measurements on the same samples. The S states were characterised by EPR measurements monitoring the S_2 multiline signal and the 'S3' signal. S_3 formation was estimated by loss of the S_2 multiline signal on illumination, decay to S_2 on thawing the sample as well as by formation of the 'S3' signal which was used as another marker for advancement above S_2. The S_1 state is EPR silent, but formation of S_2 (one flash) and S_3 (two flashes [13]) by single turnover laser flash illumination and the formation of S_2 by continuous illumination of EPR samples under conditions restricting PS II to a single turnover (0.5 mM 3-(3,4-dichlorophenyl)-1,1-dimethylurea, DCMU) was used to indicate that samples were in the S_1 state. Very similar sizes of EPR signal (using cytochrome b_{559} as a control) were seen from different preparations of each inhibitory treatment. In acetate-treated and sodium chloride-treated samples < 5%, and in ammonium chloride-treated samples < 10% total Mn was present as Mn^{2+} (EPR detectable) indicating that the integrity of the OEC was maintained. Addition of 20 mM calcium chloride to dialysed samples followed by 30 min incubation restored the normal S state turnover and S_2 multiline formation.

X-ray absorption spectroscopy

Fluorescence EXAFS [35] measurements were carried out as in [22] at the Synchrotron Radiation Source, S.E.R.C. Daresbury Laboratory, using station 8.1 with a slitless Si(220) double crystal monochromator and a thirteen element Ge solid-state detector. Spectra were recorded at 77 K with a beam energy of 2 GeV and an average beam current of 160 mA. Each scan lasted approximately 1 h. To maintain samples fully in S_3, samples were illuminated for 30 s at 77 K [17] in the EXAFS cryostat after two scans. Five scans were accumulated per sample. Comparison of the first and last scans of each sample did not reveal any change in edge position during beam exposure. Data from each of the detector elements were examined separately for anomalies and weighted by the edge-jump before averaging. Energy calibration was based on the pre-edge peak of $KMnO_4$, 6543.3 eV, and confirmed with the first inflection of the edge for Mn foil, 5 μm, 6548.0 eV. Mn K-edge energies were measured by taking the first inflection point of the rising edge. The edge measurements reported are the result of scans from at least two samples of each type of preparation in each S state. This was repeated on at least two different preparations of each inhibitory treatment to ensure reproducibility. Individual samples were generally used for a single S state measurement, but as indicated in Section 3 below, some samples were given single scans in each S state. Estimated errors in the edge measurements are ± 0.2 eV.

3. Results

The S state changes in samples were monitored by EPR in samples made in parallel with the XANES samples as described in Section 2. In native PS II membrane particles poised in the S_2 state, a multiline signal ($g = 2$, 18–20 lines, 160 mT wide, $S' = 1/2$) is normally observed. The sodium chloride- and ammonia-treated samples also exhibit a multiline signal, though it is modified to contain more hyperfine lines and is less intense [12,17,18] (Fig. 1a,b lower spectrum). The acetate-treated sample appears to have an EPR silent S_2 form, perhaps through line broadening [20]. Fig. 2 shows the light-induced EPR spectra of the S_3 states from the various preparations used in this study. In the S_3 state, each of the inhibited samples exhibits a signal near $g = 2$, with linewidth dependent on the treatment, < 10.0 mT for ammonia, 15.0 mT for sodium chloride and 24.0 mT for acetate treatment, though additional features are apparent, most obviously in the case of acetate treatment. The multiline signals observed in the S_2 state are absent or decreased several-fold in amplitude in S_3 [9–13,17].

The XANES spectra for the treated samples are shown in Figs. 3, 4 and 5 for the sodium acetate, sodium chloride and ammonia-treated samples respectively. Edge energies are shown in Table 1.

For the 600 mM acetate-treated samples at pH 5.5 (Fig. 3), a modified S_1 state is formed by treating dark adapted BBYs in the native S_1 state with a high acetate

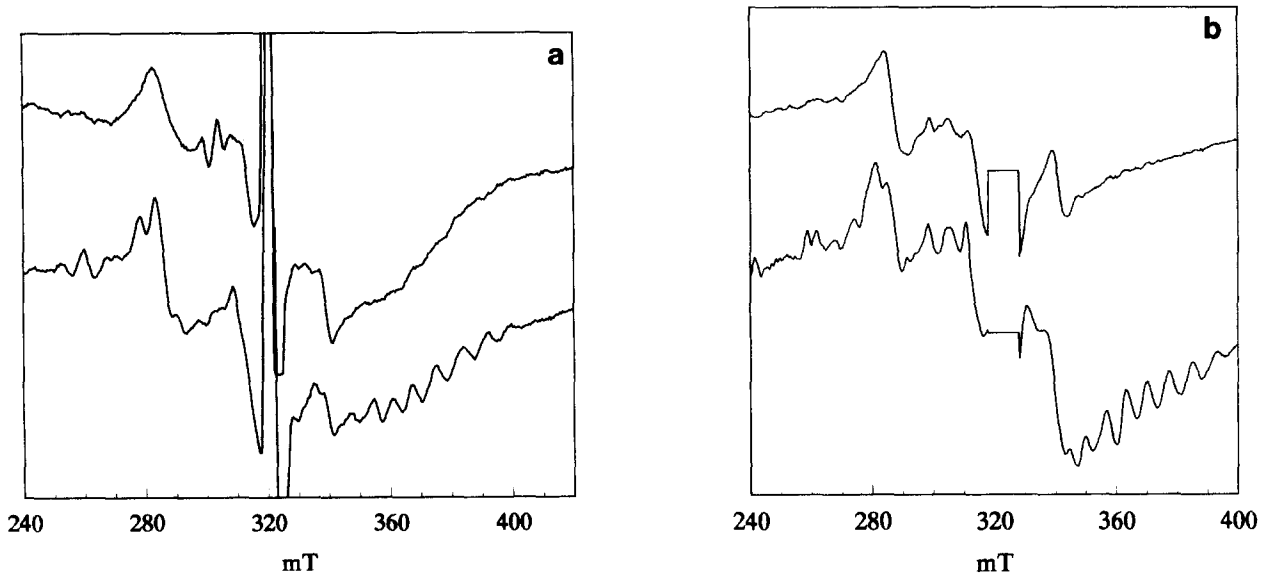

Fig. 1. X-Band EPR spectra showing the S_1 and S_2 states in (a) 600 mM sodium chloride (pH 6.0), treated sample and (b) 100 mM ammonium chloride (pH 7.5), treated sample. Upper spectra show the EPR silent S_1 state, the spectrum containing contributions from cytochrome b_{559} (280 mT) tyrosine Y_D^+ (320 mT) and the Rieske iron-sulphur centre (340 mT). The lower spectra show the additional multiline signal obtained in the S_2 state by the procedure given in Section 2. Spectrometer conditions: microwave frequency, 9.055 GHz; modulation frequency, 100 kHz; modulation amplitude, 1.6 mT; microwave power, 5 mW; temperature, 10 K.

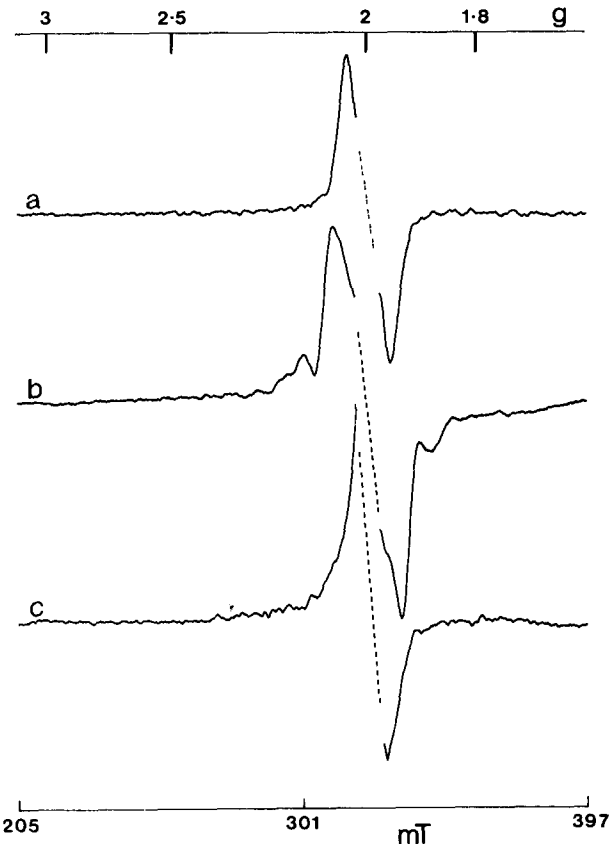

Fig. 2. X-Band EPR spectra of inhibited samples poised in the S_3 state. (a) 600 mM sodium chloride (pH 6.0), treated sample; (b) 600 mM sodium acetate (pH 5.5), treated sample: (c) 100 mM ammonium chloride (pH 7.5), treated sample. Spectrometer conditions as Fig. 1.

concentration in the dark. This has an edge energy of 6552.6 eV, approximately 1.0 eV higher than that reported for the S_1 state of the untreated membranes, 6551.4–6551.6 eV (e.g. [31]). Illumination to produce the S_3 state results in an edge energy of 6553.8 eV, 1.2 eV greater than S_1. The nominal modified S_2 state formed on 5 min dark adaption of a sample illuminated at room temperature has an edge energy of 6553.2 eV, halfway between the S_1 and S_3 states. The half-life of the 'S3' EPR signal is about 15 s at 277 K for the acetate sample [20].

For samples prepared by treatment with 600 mM sodium chloride at pH 6, there are also changes on the $S_1 \rightarrow S_3$ and $S_3 \rightarrow S_2$ transitions (Fig. 4). The S_1 dark

Table 1
Mn K-edge energies (eV)

	S_1	S_2	S_3
Intact PS II	6551.6	6552.6	–
Acetate	6552.6	6553.2	6553.8
Sodium chloride	6551.0	6551.9	6553.2
Ammonia	6550.6	6551.5	6552.5

The Table shows the edge energies for the treatments described in the text and Figs. 3–5.

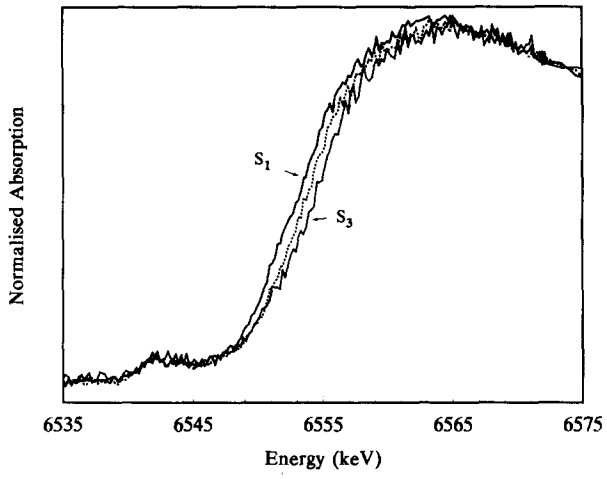

Fig. 3. Mn K-edge XANES spectra of PS II membranes treated with 600 mM sodium acetate (pH 5.5), 40 mM MES, 0.3 M sucrose. Left-hand trace, dark adapted sample, S_1; right-hand trace, sample frozen under illumination to 77 K, S_3; dashed curve, sample illuminated at 273 K for 2 min followed by a 5 min dark adaption at 273 K before freezing in the dark to 77 K, S_2.

adapted sample had an edge energy of 6551.0 eV, some 0.4–0.6 eV lower than that reported for the untreated membranes, but close to that observed by MacLachlan et al. [19,22], for NaCl-washed membranes and by Ono et al. [21], for pH 3 citrate-treated membranes. On illumination at 273 K to produce the S_3 state, the edge energy shifted to 6553.2 eV. Dark adaption for 10 min of an illuminated sample to produce modified S_2 resulted in an edge energy of 6551.9 eV.

Samples prepared in the presence of 100 mM ammonium chloride at pH 7.5 (Fig. 5), when illuminated to produce the S_3 state, gave an edge energy of 6552.5

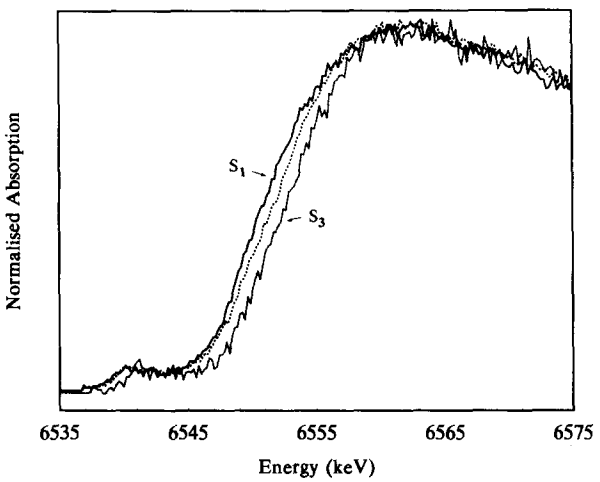

Fig. 4. Mn K-edge XANES spectra of PS II membranes treated with 600 mM sodium chloride (pH 6.0), 40 mM MES, 0.3 M sucrose. Left-hand trace, dark adapted sample, S_1; right-hand trace, sample frozen under illumination to 77 K, S_3; dashed curve, sample illuminated at 273 K for 2 min followed by a 10 min dark adaption before freezing in the dark to 77 K, S_2.

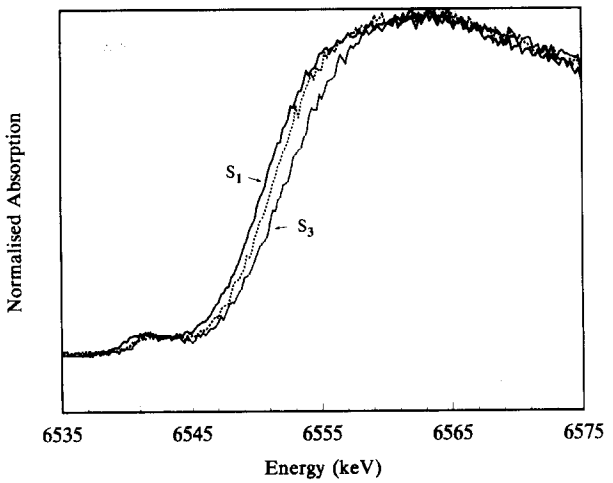

Fig. 5. Mn K-edge XANES spectra of PS II membranes treated with 100 mM ammonium chloride (pH 7.5), 20 mM Hepes, 0.3 M sucrose. Left-hand trace, dark adapted sample, S_1; right-hand trace, sample frozen under illumination to 77 K, S_3; dashed curve, sample illuminated at 273 K for 2 min followed by a 5 min dark adaption before freezing in the dark to 77 K, S_2.

eV, while the S_2 state had an edge energy of 6551.5 eV. The dark adapted S_1 state had an edge energy of 6550.6 eV.

All of the inhibition treatments studied here exhibit an 'S3' EPR signal at 10 K when poised in the S_3 state by room temperature illumination and show a downshift in the edge energy on the $S_3 \rightarrow S_2$ transition of 0.6–1.3 eV. They also have an edge energy similar to that reported recently for the S_3 state in untreated samples, 6553.3 eV [31], vs. 6552.5–6553.8 eV for the inhibited samples reported here. Single scans of a sample cycled through the S_1, S_3 and then S_2 states also showed significant edge shifts for the $S_1 \rightarrow S_3$ and $S_3 \rightarrow S_2$ transitions (not shown).

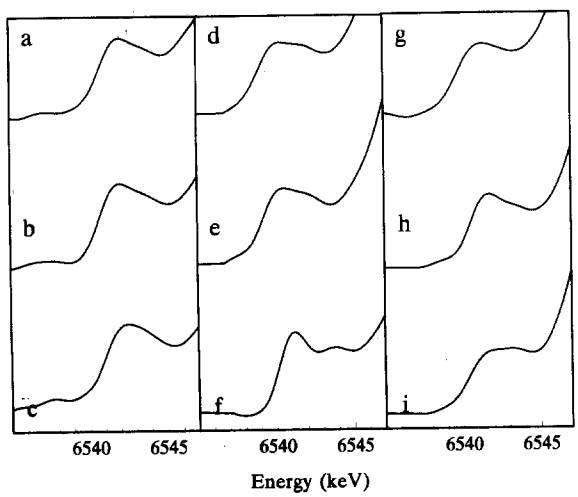

Fig. 6. The pre-edge region of the Mn K-edge spectra of inhibited PS II samples poised in the S_1 (spectra in top row), S_2 and S_3 (spectra in bottom row) states respectively; (a–c) sodium acetate-treated PS II; (d–f) sodium chloride-treated PS II; (g–i) ammonium chloride-treated PS II. Other conditions as in Figs. 3–5.

Fig. 6 shows the pre-edge features of the different samples. These pre-edge features arise from orbitally forbidden transitions, $1s \rightarrow 3d$, which gain intensity as they become weakly allowed through p-d mixing or by vibronic coupling. In general, the intensity and structure of the pre-edge features should be able to provide information on the manganese geometry, though it is also dependent on the manganese oxidation state and coordination number. The intensity follows the trend $4 > 5 > 6$ coordinate manganese in mononuclear complexes. From Fig. 6 it is apparent that there is an increase in the area of the pre-edge feature in the S_3 samples relative to those of the S_1 and S_2 states. There is also an increase in amplitude at higher energy just before the continuum threshold. Such changes are consistent with an increase in Mn oxidation, Mn(III) → Mn(IV) [36]. The shape of the pre-edge features are different for each inhibition treatment.

4. Discussion

Manganese oxidation state changes

Changes in the Mn K-edge energy can be used to determine changes occurring at the manganese cluster in inhibited samples and allow comparisons to be drawn with the intact OEC. It has been suggested that there is no oxidation of Mn in the OEC on the $S_2 \rightarrow S_3$ transition on the basis of the lack of an observed Mn K-edge shift [25,27]. This view was supported by data from relaxation measurements of Y_D^+ [28,29], from some interpretations of the optical data (e.g. [13]) and from Mn near-infrared electronic absorption measurements [38]. However, none of these experiments were conclusive.

Recent XANES measurements, on membranes poised in the different S-states by flash illumination, show an edge shift on the normal $S_2 \rightarrow S_3$ transition [31]. This questions the assumption of a lack of oxidation on the $S_2 \rightarrow S_3$ transition, although the edge shift might also be explained by structural rearrangements on this transition. Structural change associated with a protonation event or changes in the conformation of the manganese cluster has been predicted from the higher temperature required for the $S_2 \rightarrow S_3$ transition and also from activation energy estimates [39]. However, the fact that edge shifts and EPR changes are seen on each transition strongly support the proposal that net oxidation of the manganese cluster occurs on both the $S_1 \rightarrow S_2$ and $S_2 \rightarrow S_3$ transitions.

Changes in edge energy are related to both the effective nuclear charge seen by an electron on the metal and the effective charge on the metal. This depends not only on the formal oxidation state but also

depends on the ligands (covalency effects). The results presented here show similar edge shifts for the modified S_3 state to those observed in native membrane preparations [31], and a 0.5–1.3 eV upshift in edge energy for the modified $S_2 \rightarrow S_3$ transition. This may be interpreted as a manganese oxidation, although as suggested above for the native enzyme, significant structural rearrangement without an accompanying manganese oxidation could also be invoked. We consider the latter explanation unlikely as the changes in the pre-edge features for the modified $S_2 \rightarrow S_3$ transition also suggest manganese oxidation occurs and no major conformational changes are indicated by EXAFS (in preparation). If there is no manganese oxidation on the $S_2 \rightarrow S_3$ transition it is difficult to understand why a major rearrangement of the manganese cluster would occur. The previous failure to observe an edge shift was taken as evidence that no redox change occurred in the manganese complex on the $S_2 \rightarrow S_3$ transition [25,27]. The observation here of an edge shift suggests that manganese oxidation does occur on $S_2 \rightarrow S_3$ in our inhibited samples.

Interpretation of the edge shifts as indicating manganese oxidation on the $S_2 \rightarrow S_3$ transition would be consistent with other data such as the observations of van Leeuwen et al. [41]. They reinterpret the optical data of Boussac et al. [13], showing that the spectra obtained could be of manganese oxidation on the $S_2 \rightarrow S_3$ transition and not oxidation of histidine radical. A manganese oxidation would also account for the differences in saturation behaviour of Y_D^+ observed for inhibited samples in the modified S_2 and S_3 states [17].

Conformational changes

An understanding of the structure of the manganese complex in PS II is complicated by the existence of more than one conformation in the S_1 and S_2 states. Several studies have suggested active/inactive conformations for the native S_1 state [39,42,43], in addition to at least three conformations proposed for S_2, each having a characteristic EPR signal, i.e., the $g = 2$ multiline, $g = 4.1$ and an EPR silent form (see [1,2] for reviews). The three types of inhibited sample have different edge energies for the dark S_1 states compared to untreated membranes (-0.6 eV for sodium chloride, -1.0 eV for ammonia and $+1.0$ eV for acetate). The changes can arise either from differences in coordination geometry and/or ligands or from oxidation state changes. One electron reduction or oxidation of the native S_1 state, which may be either $Mn(III)_4$ or $Mn(III)_2$ $Mn(IV)_2$, would be expected to produce an EPR active complex in the modified S state. EPR spectra of the S_1 states of the inhibited samples do not reveal any new signals that might be expected on the reduction or oxidation of the EPR silent native S_1 state. Therefore the variation in the edge energies of a particular S-state following different inhibitory treatments are probably not due to redox changes but arise from slight structural differences in the conformation and/or ligands to the manganese cluster. Evidence for such conformational and/or ligand changes can be observed by EPR. The EPR signals in the S_2 and S_3 states for the different treatments show that different S_2 multilines are observed for sodium chloride- [9,12] and ammonia-treated PS II [44], while acetate treatment results in what appears to be an EPR silent conformation for the S_2 state [20]. In the S_3 state, the linewidths observed for the broad $g = 2$ signals are also different, Hpp 24.0 mT for acetate, 15.0 mT for sodium chloride and < 10.0 mT in the case of ammonium chloride. The differences in the pre-edge features of inhibited samples in a given S-state also indicate structural differences.

Both calcium and chloride are required for oxygen evolution. It is tempting to interpret the changes in edge energy following ammonia or acetate treatment as indicating direct binding of chloride, or competitive inhibitors, to the manganese cluster (see [1,2] for reviews). Calcium could similarly be suggested to share ligands with the manganese cluster, e.g., a carboxylate bridging ligand. This would agree with suggestions that calcium might be a scatterer involved in the 3.3–3.6 Å or 4.3 Å distances observed in EXAFS studies [22,37].

Possible roles for calcium and chloride include (1) control of substrate accessibility, (2) modulation of the redox potential of the manganese cluster or (3) involvement in proton transfer. That the roles proposed for both cofactors are similar is due to our limited understanding of water oxidation and the effects of depletion/inhibition treatments. It is apparent from EPR and thermoluminescence studies [9–11] that the modified S_2 states of the inhibited samples are stabilised compared to the untreated S_2 state. Lowering of the cluster oxidation potential to < 0.8 V would inactivate water oxidation without affecting Y_Z function.

The origin of the 'S3' EPR signal

It has been proposed that the signal arises, following oxidation of the OEC from the S_2 state, from an interaction between the S_2 state and an organic radical, S_2 X^+ [9,13,17,20]. If manganese is oxidised on the $S_2 \rightarrow S_3$ transition, this explanation cannot be correct. The Curie temperature dependence of the 'S3' EPR signal between 4–20 K [9,45] indicates an isolated doublet ground state, typical of a $S = 1/2$ spin system or of a $S > 1/2$ system without any low-lying excited states. Strong relaxation is also observed for this signal, e.g., $P_{\frac{1}{2}} > 1$ mW at 10 K, suggesting the involvement of a transition metal, compatible with the signal arising from the manganese cluster of PS II. The signal then might arise from exchange coupling between two man-

ganese $S' = 1/2$ systems, reflecting the two pairs of oxo-bridged manganese dimers thought to form the complex. In the case of two exchange-coupled manganese $S' = 1/2$ systems with weak coupling, the explanation for the observed EPR signals is not much changed from the S_2 X^+ radical proposal, except that the two interacting species are both manganese. However, it has been proposed that the 'S3' is formed in less than 25% of the reaction centres in pH 3 citrate washed PS II [40], although the S_2 multiline is absent which indicates an oxidation from S_2 occurs in most centres. This implies most of the centres have an EPR silent S_3 state. Secondly, the linewidth of the 'S3' EPR signal at $g = 2$, < 250 Gauss is not matched by those of known manganese complexes, approx. 500–2800 Gauss. The results could be explained if the inhibitory treatments allow S state advancement from S_2 to S_3 except that the kinetics of formation/decay allow S_2 X^+ to form in a proportion of centres, giving rise to the 'S3' EPR signal, perhaps as an intermediate state in redox equilibrium with S_3. We are currently attempting to simulate and quantitate the 'S3' EPR signal observed in acetate-treated and calcium-depleted samples in order to better define this state.

Conclusion

In order to explain the lack of evidence for Mn oxidation on the $S_2 \rightarrow S_3$ transition, it was proposed that some other species was oxidized, i.e., an amino acid. The data presented here are the first evidence supporting manganese oxidation on the S_2 to S_3 transition in samples where the S_3 to S_0 transition is inhibited. From the changes in edge energy on inhibition/depletion of cofactors, it appears that both chloride and calcium are intimately associated with the manganese cluster.

5. Acknowledgements

We wish to thank Dr. Samar Hasnain, Dr. Richard Strange, Dr. Margaret Neu, Menno Oversluizen and Lorrie Murphy at the SRS Daresbury for their help. We also wish to thank Professor Joseph Warden and Dr. Stephen Rigby for helpful comments and discussion. We acknowledge financial assistance from the UK Science and Engineering Research Council.

6. References

[1] Debus, R.J. (1992) Biochim. Biophys. Acta 1102, 269–352.
[2] Rutherford, A.W., Zimmermann, J.-L. and Boussac, A. (1992) in The Photosystems: Structure, Function and Molecular Biology, (Barber, J. ed.), Chapter 5, pp. 179–229, Elsevier, Amsterdam.
[3] Coleman, W.J. (1990) Photosynth. Res. 23, 1–27.
[4] Yocum, C.F. (1991) Biochim. Biophys. Acta 1059, 1–15.
[5] Ghanotakis, D.F., Babcock, G.T. and Yocum, C.F. (1984) FEBS Lett. 167, 127–130.
[6] Pistorius, E.K. (1983) Eur. J. Biochem. 135, 217–222.
[7] Damoder, R., Klimov, V.V. and Dismukes, G.C. (1986) Biochim. Biophys. Acta 848, 378–391.
[8] Dismukes, G.C. and Siderer, Y. (1980) FEBS Lett. 121, 78–80.
[9] Boussac, A., Zimmermann, J.-L. and Rutherford, A.W. (1989) Biochemistry 28, 8984–8989.
[10] Sivaraja, M., Tso, J. and Dismukes, G.C. (1989) Biochemistry 28, 9459–9464.
[11] Ono, T. and Inoue, Y. (1990) Biochim. Biophys. Acta 1020, 269–277.
[12] Boussac, A., Zimmermann, J.-L. and Rutherford, A.W. (1990) FEBS Lett. 277, 69–74.
[13] Boussac, A., Zimmermann, J.-L., Rutherford, A.W. and Lavergne, J. (1990) Nature 347, 303–306.
[14] Kirilovsky, D.L., Boussac, A., Van Mieghem, F.J.E., Ducruet, J.-M.R.C., Setif, P.R., Yu, J., Vermaas, W.F.J. and Rutherford, A.W. (1992) Biochemistry 31, 2099–2107.
[15] Baumgarten, M., Philo, J.S. and Dismukes, G.C. (1990) Biochemistry 29, 10814–10822.
[16] Boussac, A., Setif, P. and Rutherford, A.W. (1992) Biochemistry 31, 1224–1234.
[17] Hallahan, B.J., Nugent, J.H.A., Warden, J.T. and Evans, M.C.W. (1992) Biochemistry 31, 4562–4573.
[18] Andreasson, L.-E. and Lindberg, K. (1992) Biochim. Biophys. Acta 1100, 177–183.
[19] MacLachlan, D.J., Nugent, J.H.A. and Evans, M.C.W. (1992) in Research in Photosynthesis (Murata, N., ed.), Vol II, pp. 373–380, Kluwer, Dordrecht.
[20] MacLachlan, D.J. and Nugent, J.H.A. (1993) Biochemistry 32, 9772–9780.
[21] Ono, T., Kusunoki, M., Matsushita, T., Oyanagi, H. and Inoue, Y. (1991) Biochemistry 30, 6836–6841.
[22] MacLachlan, D.J., Hallahan, B.J., Ruffle, S.V., Nugent, J.H.A., Evans, M.C.W., Strange, R.W. and Hasnain, S.S. (1992) Biochem. J. 285, 569–576.
[23] Yachandra, V.K., Guiles, R.D., McDermott, A.E., Britt, R.D., Dexheimer, S.L., Sauer, K. and Klein, M.P. (1986) Biochim. Biophys. Acta 850, 324–332.
[24] Guiles, R.D., Yachandra, V.K., McDermott, A.E., Cole, J.L., Dexheimer, S.L., Britt, R.D., Sauer, K. and Klein, M.P. (1990) Biochemistry 29, 486–496.
[25] Goodin, D.B., Yachandra, V.K., Britt, R.D., Sauer, K. and Klein, M.P. (1984) Biochim. Biophys. Acta 767, 209–216.
[26] Kusunoki, M., Ono, T., Matsushita, T., Oyanagi, H. and Inoue, Y. (1990) J. Biochem. 108, 560–567.
[27] Guiles, R.D., Zimmermann, J-L., McDermott, A.E., Yachandra, V.K., Cole, J.L., Dexheimer, S.L., Britt, R.D., Wieghardt, K., Bossek, U., Sauer, K. and Klein, M.P. (1990) Biochemistry 29, 471–485.
[28] Styring, S.A. and Rutherford, A.W. (1988) Biochemistry 27, 4915–4923.
[29] Evelo, R.G., Styring, S.A., Rutherford, A.W. and Hoff, A.J. (1989) Biochim. Biophys. Acta 973, 428–442.
[30] Sharp, R.R. (1992) in Manganese Redox Enzymes (Pecoraro, V.L., ed.), pp 177–196, VCH, New York.
[31] Ono, T., Noguchi, T., Inoue, Y., Kusunoki, M., Matsushita, T. and Oyanagi, H. (1992) Science 258, 1335–1337.
[32] Berthold, D.A., Babcock, G.T. and Yocum, C.F. (1981) FEBS Lett. 134, 231–234.
[33] Ford, R.C. and Evans, M.C.W. (1983) FEBS Lett. 160, 159–163.
[34] Saygin, O., Gerken, S., Meyer, B. and Witt, H.T. (1986) Photosynth. Res. 9, 71–78.
[35] Hasnain, S.S., Quinn, P.D., Diakun, G.P., Wardell, E.M. and Garner, C.D. (1984) J. Phys. E. Sci. Instrum. 17, 40–43.

[36] Manceau, A., Gorshkov, A.I. and Drits, V.A. (1992) Am. Miner. 77, 1133–1143.
[37] Penner-Hahn, J.E., Fronko, R.M., Pecoraro, V.L., Yocum, C.F., Bretts, S.D. and Bowlby, N.R. (1990) J. Am. Chem. Soc. 112, 2549–2557.
[38] Dismukes, G.C. and Mathis, P. (1984) FEBS Lett. 178, 51–54.
[39] Renger, G. and Hanssum, B. (1992) FEBS Lett. 299, 28–32.
[40] Gilchrist, M.L., Lorigan, G.A. and Britt, R.D. (1992) in Research in Photosynthesis (Murata, N., ed.), Vol II, pp. 317–320, Kluwer, Dordrecht.
[41] Van Leeuwen, P.J., Van Gorkom, H.J. and Dekker, J.P. (1992) J. Photochem. Photobiol. 15, 33–43.
[42] Beck, W.F., De Paula, J.C. and Brudvig, G.W. (1985) Biochemistry 24, 3035–3043.
[43] Koulougliotis, D., Hirsh, D.J. and Brudvig, G.W. (1992) J. Am. Chem. Soc., 114, 8322–8323.
[44] Beck, W.F., De Paula, J.C. and Brudvig, G.W. (1986) J. Am. Chem. Soc. 108, 4018–4022.
[45] Tso, J., Sivaraja, M., Philo, J.S. and Dismukes, G.C. (1991) Biochemistry 30, 4740–4747.